Atmospheric Environment 235 (2020) 117624

Contents lists available at ScienceDirect

Atmospheric Environment

journal homepage: http://www.elsevier.com/locate/atmosenv

Short communication

Source apportionment of water-soluble oxidative potential in ambient total suspended particulate from Bangkok: Biomass burning *versus* fossil fuel combustion

Jiaqi Wang [a,b], Haoyu Jiang [a,b], Hongxing Jiang [a,b], Yangzhi Mo [a,b], Xiaofei Geng [a,b], Jibing Li [a,b], Shuduan Mao [a,b], Surat Bualert [c], Shexia Ma [d], Jun Li [a], Gan Zhang [a,*]

[a] State Key Laboratory of Organic Geochemistry and Guangdong Key Laboratory of Environmental Protection and Resources Utilization, Guangzhou Institute of Geochemistry, Chinese Academy of Sciences, Guangzhou, 510640, China
[b] University of Chinese Academy of Sciences, Beijing, 100039, China
[c] Faculty of Environment, Kasetsart University, Bangkok, 10900, Thailand
[d] South China Institute of Environmental Sciences, Ministry of Environmental Protection, Guangzhou, 510655, China

HIGHLIGHTS

- Chemical composition and OP of ambient TSP from Bangkok were measured.
- Averaged chemical species and OPv peaked in dry seasons.
- OPm decreased as TSP concentration increased due to the unaccounted fractions dominating the increase in TSP and/or the inhibiting effects of redox-active metals.
- OPm significantly correlates with transition metals, hopanes/steranes, and OC/EC.
- OPv of TSP is driven by transition metals from fossil fuel combustion, albeit extensive regional biomass burning.

GRAPHICAL ABSTRACT

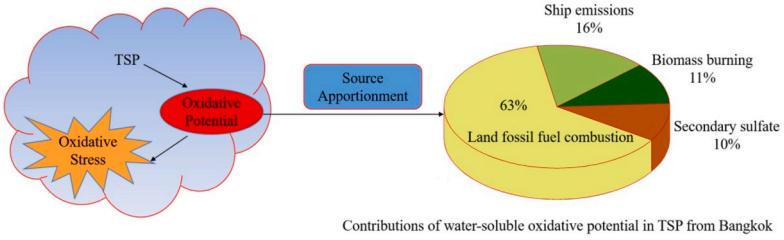

Contributions of water-soluble oxidative potential in TSP from Bangkok

ARTICLE INFO

Keywords:
Indochinese peninsula
Metals
Oxidative potential
Source apportionment
TSP

ABSTRACT

Oxidative potential (OP) is a promising and integrative metric for assessing health effects associated with exposure to ambient particulate matter. Source apportionment of water-soluble OP in aerosols is the basis for formulating pollution control policies. In this study, we collected total suspended particulate (TSP) samples in Bangkok, on the Indochinese Peninsula, where pollution levels are high due to annual biomass burning. We analyzed the chemical composition of the samples and performed dithiothreitol (DTT) assays to measure their OP. We observed higher TSP mass and chemical species concentrations among samples collected in the dry seasons due to biomass burning and fossil fuel combustion. The seasonally averaged volume-normalized OP (OP_v) was highest in the dry I season (January to March), which was consistent with higher TSP concentrations during this period. The mass-normalized OP (OP_m) decreased as TSP concentration increased due to the unaccounted fractions dominating the increase in TSP and/or the inhibiting effects of redox-active metals. Transition metals (e.g., Cu, V, and Ni), hopanes/steranes, and carbonaceous species (organic carbon and elemental carbon)

* Corresponding author.
E-mail address: zhanggan@gig.ac.cn (G. Zhang).

https://doi.org/10.1016/j.atmosenv.2020.117624
Received 16 November 2019; Received in revised form 11 May 2020; Accepted 18 May 2020
Available online 24 May 2020

correlated well with OP_m. Source apportionment using the Positive Matrix Factorization model (PMF) and multiple linear regression analysis revealed that, although biomass burning accounted for the highest contribution (mean: 26%) to TSP concentration, the dominant source of water-soluble OP_v of TSP was fossil fuel combustion, which included land fossil fuel combustion (63%) and ship emissions (16%). This significant contribution of fossil fuel combustion was determined by the transition metals Cu and V which were the main drivers of DTT activity in TSP.

1. Introduction

The association between elevated airborne particulate matter (PM) concentration and negative health effects can lead to increased morbidity and mortality due to cardiopulmonary diseases in polluted regions (Ayres et al., 2008; Liu et al., 2014; Pavagadhi et al., 2013). One hypothesis is that many adverse health effects originate from oxidative stress induced by reactive oxygen species (ROS) at the surface of and within target cells (Ayres et al., 2008). The formation of excessive ROS breaks the redox status, inducing the oxidative stress and resulting in cell death, biological aging, and various diseases (Patel and Rastogi, 2018b; Shiraiwa et al., 2012). ROS typically includes the superoxide anion ($O^-_2\cdot$), hydrogen peroxide (H_2O_2), and hydroperoxyl ($HO_2\cdot$) and hydroxyl (·OH) radicals (Shiraiwa et al., 2012). The capacity of PM to generate ROS is defined as oxidative potential (OP). OP is considered to incorporate the health-relevant fraction of PM and provides a more refined metric than PM mass concentration or the content of specific chemical components (Fang et al., 2015).

A variety of acellular and cellular methods have been developed to quantify the OP of PM (Ayres et al., 2008). Acellular methods require a less controlled environment and provide a more rapid OP readout. The dithiothreitol (DTT) assay is the most widely employed method. This assay is based on the catalytic ability of active redox species associated with PM to transfer electrons from DTT to oxygen, where DTT is used as a surrogate for biological reducing agents (e.g., NADPH). The rate of this reaction is monitored in terms of DTT consumption, which is proportional to the OP of PM (Lin and Yu, 2011). Various chemical components have been demonstrated to be DTT-active, including some transition metals (e.g., V, Ni, and Cu), quinones, and humic-like substances (HULIS) (Lin and Yu, 2011; Verma et al., 2014). However, the complexities of PM chemical composition and their potential compounding effects make it unrealistic to attribute OP to any individual constituent (Zhang et al., 2008). There is an urgent need to directly link urban/regional aerosol OP and emission sources to establish operable risk mitigation policies. Recent studies have reported that OP was the highest for chemical species originating from vehicular exhaust, biomass burning, and road dust (Bates et al., 2019; Brehmer et al., 2019; Saffari et al., 2013). Exposure to these emissions has been linked to adverse human health endpoints including pneumonia, chronic obstructive pulmonary disease, and lung cancer (Brauner et al., 2008; Thorpe and Harrison, 2008; Zelikoff et al., 2002).

The Indochinese Peninsula (ICP) has high population densities and suffers severe biomass smoke pollution originating from seasonal biomass burning activities (Yadav et al., 2017). Most studies of the effects of biomass smoke pollution have focused on PM mass concentration and chemical composition in the ICP, whereas data on the OP of aerosols in the ICP remain scarce. In this study, to assess the relative contribution of regional biomass burning to human health, we investigated the contributions of various emission sources to the OP of aerosols in Bangkok, Thailand. To our knowledge, this is the first study on OP in PM of Bangkok.

2. Materials and methods

2.1. Sample collection

We collected 24-h total suspended particulate (TSP) samples on quartz fiber filters (203 × 254 mm, pre-combusted at 450 °C for 6 h; Munktell) using a high-volume air sampler (300 L/min; XTrust Instruments Co., Shanghai, China). The sampling site was located on the roof (height: 57 m) of the faculty of environment of Kasetsart University (13°85′N, 100°57′E). The site is located approximately 13.2 km northeast of central Bangkok; no biomass burning activity has been observed near the site. Sampling campaigns were conducted during three seasons, including the dry I season (January to March 2016), the wet season (April to June and October 2016), and the dry II season (November 2016 to January 2017). We collected 86 TSP samples and four filed blank samples using quartz filters that had been prebaked at 450 °C for 6 h. All samples were wrapped in aluminum foil and stored at −20 °C until analysis. Before and after sampling, filters were conditioned for 48 h at 25 °C and 40% humidity, and weighed on a microbalance to obtain ambient TSP concentration (μg m^{-3}).

2.2. Chemical analyses

2.2.1. Water-soluble ions, trace elements, organic carbon (OC), and elemental carbon (EC)

Details of the sample treatment and analytical method are described in Supporting Information S1. Briefly, water-soluble ions (Cl^-, NO_3^-, SO_4^{2-}, Na^+, K^+, NH_4^+, Mg^{2+}, and Ca^{2+}) were extracted from the samples with ultrapure water (18.2 MΩ; Sartorius) and measured using ion chromatography (761 Compact IC; Metrohm, Herisau, Switzerland). One punch from each filter was digested in concentrated nitric acid (ultrapure) and analyzed for trace elements using inductively coupled plasma–mass spectrometry (ICP–MS; ELAN DRC II, PerkinElmer Ltd., Hong Kong). In this study, we report only relevant elements that were expected to indicate specific emission sources. OC and EC in the samples were determined using an OC/EC analyzer (Sunset Laboratories, Tigard, OR, USA) following National Institute of Occupational Safety and Health (NIOSH) method 870.

2.2.2. Organic compounds

Detailed methods for the extraction, derivatization, and gas chromatography (GC)–MS analyses were described previously (Geng et al., 2019; Mao et al., 2018). Briefly, a section of each filter was spiked with ^{13}C-labeled levoglucosan as a recovery standard. We then performed Soxhlet extraction for 36 h with a mixture of dichloromethane (DCM) and methanol (40:3 by volume) to analyze anhydrosugars. The extracts were anhydrated with anhydrous sodium sulfate column, spiked with methyl β-D-xylopyranoside as an internal standard, and then blow-dried in a gentle nitrogen stream. After reaction with N,O-bis(trimethylsilyl) trifluoroacetamide (1% trimethylsilyl chloride) and pyridine at 70 °C for 1 h, the resulting solution was immediately analyzed using GC–MS (7890/5975; Agilent, Santa Clara, CA, USA).

A subsample was spiked with perdeuterated tetracosane as a recovery standard and extracted in Soxhlet for 36 h with a mixture of DCM and methanol (40:3 by volume). The extracts were further purified on a multilayer neutral silica gel column. Hexamethylbenzene was added as an internal standard, and five hopanes and five steranes were then quantified by GC–MS (GC-MS-QP2010; Shimadzu, Kyoto, Japan).

The method detection limit (MDL) was defined as the average of all blanks plus 3 times the standard deviation. The MDLs of each target compound are listed in Table S2. In this study, laboratory and field blanks were extracted and analyzed as normal samples using the same

solvent and analytical procedures to assess any contamination during the experimental procedures. The average recovery of three anhydrosugars (^{13}C-labeled levoglucosan) was 87% ± 10%, and that of hopanes/steranes (perdeuterated tetracosane) was 114% ± 11%. All organic tracers were corrected according the recoveries of the corresponding surrogate standards.

2.3. DTT assay

The OP of PM, estimated by the DTT assay method, can be expressed in two ways: mass-normalized OP (pmol DTT min^{-1} μg^{-1} PM, or OP_m) or volume-normalized OP (nmol DTT min^{-1} m^{-3} of air sample, or OP_v) (Charrier and Anastasio, 2012; Charrier et al., 2015; Li et al., 2009). We followed the standard DTT procedure of Perrone et al., with an additional step of treating phosphate buffer solutions with Chelex 100 resin to reduce the background oxidation of transition metals (Ayres et al., 2008; Charrier and Anastasio, 2012; Perrone et al., 2016). Briefly, one punch from each filter was extracted with ultrapure water; the extract was further filtered through a polytetrafluoroethylene membrane (0.45 μm; Anpel, Shanghai, China), mixed with DTT, and incubated at pH 7.4 and 37 °C. At known intervals, small aliquots were withdrawn from the mixture to determine the concentration of the remaining DTT using a light absorption method. The detailed DTT assay procedure is provided in Supporting Information S2.

The final DTT consumption rates of each sample were determined as OP_m (pmol DTT min^{-1} μg^{-1} PM) and OP_v (nmol DTT min^{-1}m^{-3} of air sample) as follows:

$$OP_m = \frac{\text{Blank} - \text{corrected rate of loss Ypmol DTT min}^{-1}\text{Y}}{\text{PM mass added to the tube}} \quad (1)$$

$$OP_v = \frac{OP_m \times \text{PM mass}_{\text{sample}}(\text{g})}{\text{Air volume for sampling}} \times 1000 \quad (2)$$

2.4. Statistical and spatial analyses

To assess the impacts of atmospheric transport of anthropogenic or natural emissions from surrounding areas as a potential source of TSP, we calculated 72-h backward trajectories at 6-h intervals using the Hybrid Single-particle Lagrangian Integrated Trajectory (HYSPLIT) model (http://ready.arl.noaa.gov/HYSPLIT.php). All individual trajectories were clustered for each season (Fig. 1). We used the Positive Matrix Factorization (PMF) recommended by the United States Environmental Protection Agency (US EPA) to identify and apportion ambient TSP pollution sources, as described in Supporting Information S3.

The relationship between the chemical species in TSP and OP_m was examined using Pearson correlation to determine which chemical species were significantly correlated with the measured OP, which was used as a source marker to select species to be included in the PMF model. We graded the strength of the correlation in terms of the Pearson correlation coefficient (r) as follows: $r \leq 0.3$, negligible; $0.3 < r \leq 0.5$, weak; $0.5 < r < 0.7$, moderate; and $r \geq 0.7$, strong (Brehmer et al., 2019).

The PMF and multiple linear regression (MLR) models were used jointly to quantify the individual contribution of TSP emission sources to water-soluble OP. The mass concentration of TSP as a total variable

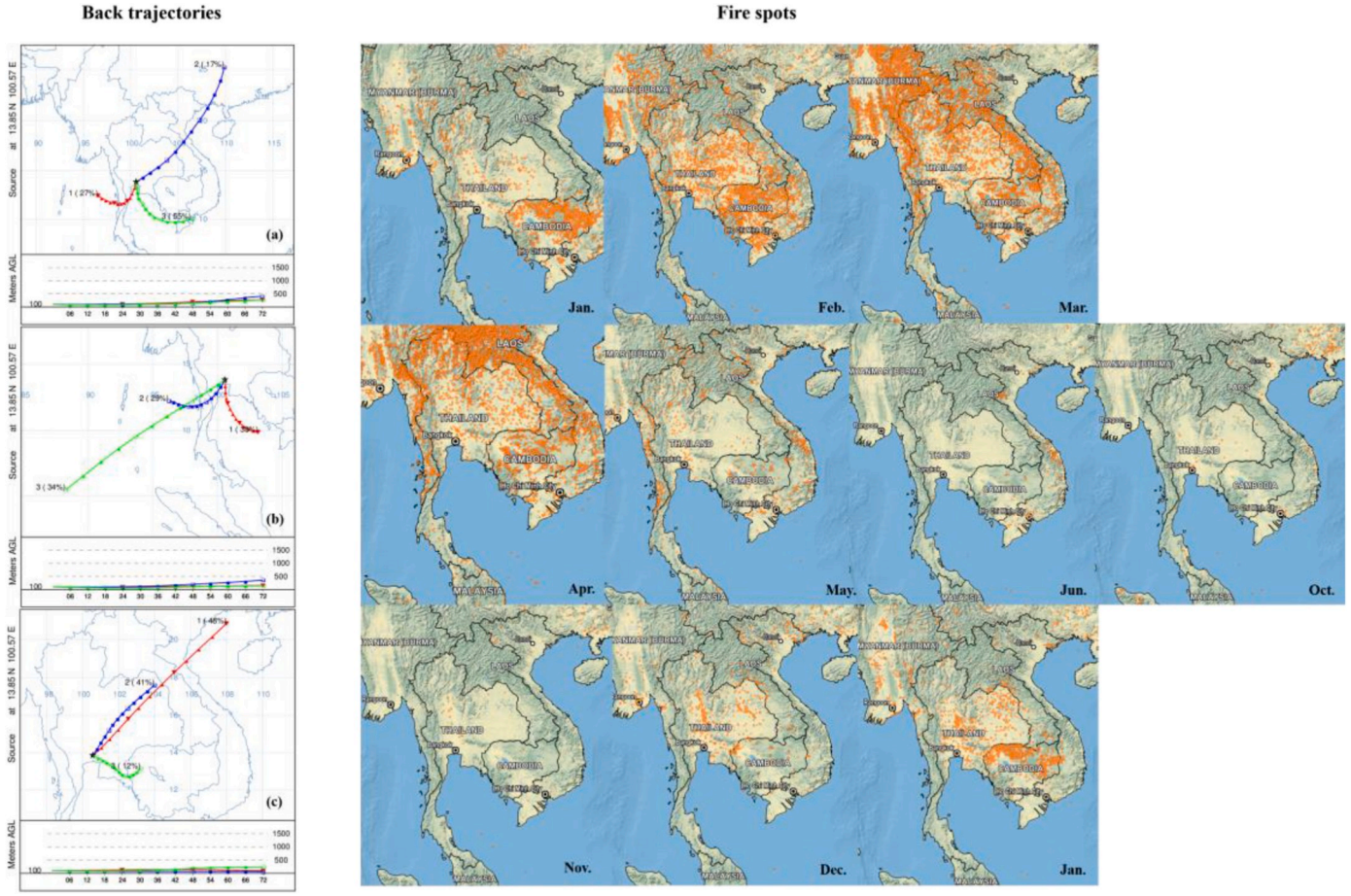

Fig. 1. Back trajectories in (a) Dry I season (January to March 2016), (b) Wet season (April to October 2016), (c) Dry II season (November 2016 to January 2017). The spatial distribution of fire spots from January 2016 to January 2017 over Thailand (https://ready.arl.nasa.gov/archieves.php).

together with chemical composition data on TSP were subjected to PMF analysis to obtain the quantitative contributions of different emission sources to the TSP mass concentration. MLR analysis was then performed for all PMF-derived source contributions (independent variables, μg m^{-3}) and the corresponding OP_v data (dependent variable, nmol DTT min^{-1} m^{-3}). Next, MLR-identified emission sources that contributed significantly to the OP of TSP were identified using a stepwise screening process. The MLR equation was then established to account for the contribution of each source to OP.

3. Results and discussion

3.1. Temporal variations in chemical composition

As shown in Fig. 2, the four main components (organic matter [OM, estimated as 1.6 times that of OC], EC, water-soluble ions and trace elements) accounted for 66%, 73% and 61% of TSP during the dry I season, wet season, and dry II season, respectively (Xing et al., 2013). Among the unaccounted fractions (the difference between TSP concentration and the sum of the remaining fractions), relative contributions ranged from 28% to 39% throughout the sampling period. The unaccounted fraction has different origins, such as the undissolved components of silicates, underestimations of the OM fraction, or water bound to secondary inorganic aerosols (Pey et al., 2010). The mean TSP concentrations during the dry I and dry II seasons were nearly 2 fold higher than that of the wet season. Similar seasonal variations were observed for each species, with higher concentrations during dry seasons than in the wet season (Table S3).

The 72-h backward trajectories (Fig. 1) showed that, during the dry seasons, air masses passed over the continental regions of northeastern Thailand and southwestern Cambodia. Moderate Resolution Imaging Spectroradiometer (MODIS) firespot maps revealed widespread open biomass burning. Larger amounts of pollutants are generated during such massive biomass burning periods in Southeast Asia (Tang et al., 2007). In Bangkok, far greater EC levels were observed in both dry seasons than in the wet season (Table S3). EC originates primarily from anthropogenic sources, typically including fossil fuel combustion and biomass burning (Zhang et al., 2014). These results suggest that higher concentrations of TSP and chemical species could be attributed to biomass burning and fossil fuel combustion. During the wet season, air masses mainly originated from the Gulf of Thailand and Andaman Sea. The low concentrations observed in the wet season were likely due to clean air masses originating from marine areas, together with abundant precipitation (Zhang et al., 2010).

3.2. OP of TSP

Table S3 shows OP_v and OP_m during the dry I season, the wet season, and the dry II season in Bangkok. OP_v varied from 1.25 to 3.82 nmol DTT min^{-1} m^{-3} (mean, 2.23), which was similar to the seasonal trend of TSP concentration, and seasonal averages peaked in the dry I season, followed by the dry II season and the wet season. OP_v is a reasonable unit for air pollution exposure assessment; therefore, we compared our OP_v values to those of previous studies performed in cities of China (Yu et al., 2019) and India (Patel and Rastogi, 2018a) using the same analytical method (Table 1). OP_v was 1.7- and 2.1-fold higher for these cities than our result, respectively. The corresponding PM concentrations were 2.6- and 2.0-fold higher than that of the present study, respectively. The lower OP_v may therefore be attributed to lower TSP mass concentration over the study region compared to these previous studies. As shown in Fig. 3a, OP_v was strongly dependent on TSP concentration, especially at lower concentrations; however, the increasing trend approached a plateau when TSP concentration increased to higher levels, indicating that the DTT consumption rate decreases as PM concentration increases.

On a per PM mass basis, OP_m varied from 18.5 to 119 pmol DTT min^{-1} μg^{-1} (mean, 48.1), which was similar or somewhat lower than values observed in Japan (Fujitani et al., 2017), Europe (Janssen et al., 2014), and the United States (Charrier et al., 2015; Saffari et al., 2014b) (Table 1). This finding suggests that, even assuming that particles of different size have equal mass, the OP_m of TSP would be lower than that of coarse or fine particles. Generally, OP_m decreases with increasing particle size, and ultrafine particles usually exhibit much higher OP_m than accumulation or coarse particles (Bates et al., 2019). This phenomenon is likely due to the different dominant DTT-active components in particles of different size. For coarse particles, water-soluble OP is mainly associated with transition metal ions (Fang et al., 2017b). In the present study, a power function was observed between OP_m and TSP mass concentration (Fig. 3b). There are two possible reasons for this observed pattern. One is that the increased mass of TSP has little influence on OP_m. The unaccounted fractions dominated the increase in TSP in both the dry I (43.3%) and dry II season (48.5%), whereas they did not contribute to water-soluble OP according to the DTT assay. The second possibility is the inhibiting effect of high levels of redox-active metals in the DTT assay. Charrier et al. investigated the DTT responses of hypothetical and ambient PM samples, and found that this pattern was driven by a non-linear Cu concentration response (Charrier et al., 2016). In another study a DTT assay was performed to examine the specific suppression effect in a Cu–HULIS mixture; the results suggested that organic ligands in HULIS are likely involved in some steps of Cu-catalyzed DTT oxidation, thereby resulting in suppressed DTT oxidation (Lin and Yu, 2019). Because Mn and V have a size distribution similar to that of Cu, they may be involved the same processes, shaping the water-soluble OP of TSP. Therefore, future study is needed to further investigate the inhibiting effect of transition metals in TSP.

3.3. Source apportionment of water-soluble OP in TSP from Bangkok

3.3.1. Correlation between individual species and OP

Pearson correlation analysis was used to investigate potential correlations between OP_m (μg^{-1}) and select chemical species (μg^{-1}); the

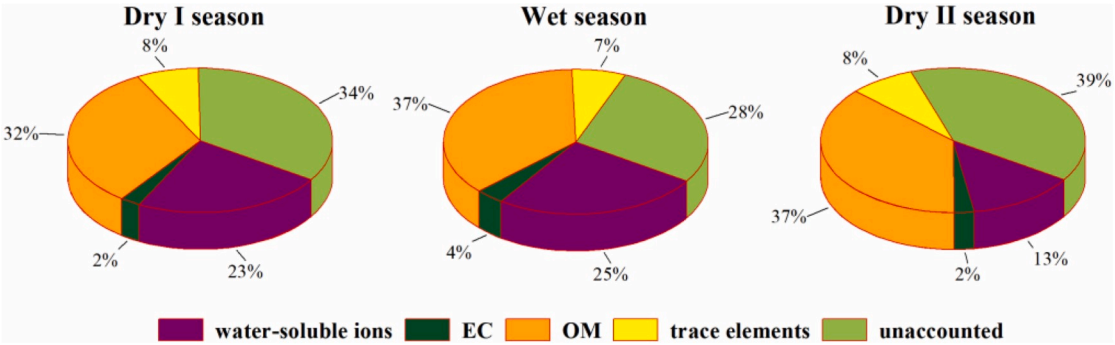

Fig. 2. Chemical composition of TSP in Bangkok during the sampling period.

Table 1
Comparison that applied DTT assay for the assessment of the oxidative potential of particulate matter (PM) normalized by air volume (OP_v, left panels), and PM mass (OP_v, right panels).

Sampling site	the volume-normalized OP (nmol DTT $min^{-1}m^{-3}$, OP_v)				the mass-normalized OP (pmol DTT min^{-1} μg^{-1} PM, OP_m)			
	TSP≤ μ100 μm	coarse 2.5–10 μm	Fine ≤ 2.5 μm	ultrafine≤ 1.0 μm	TSP≤ 100 μm	coarse 2.5–10 μm	fine≤ μ2.5 μm	ultrafine≤ 1.0 μm
Bangkok[a]	2.23 ± 0.61				48.1 ± 20.8			
Patiala[b]			3.8 ± 1.4				27 ± 8	
Beijing[c]			4.67 ± 1.06				130 ± 100	
Traffic intersection, Japan[d]							50.9 ± 27.8	
Continuous traffic, Netherlands[e]		3.54	2.78			89	119	
Farm, Netherlands[e]		3.19	2.94			58	82	
Los Angeles central-annual avg[f]								78.5 ± 8.0
Los Angeles west-annual avg[f]								46.0 ± 16.5
Los Angeles east-annual avg[f]								66.7 ± 18.5
Fresno, CA-summer ave[g]							80	48
Fresno, CA-winter ave[g]							50	39

[a] (Present study, Bangkok).
[b] (Patel and Rastogi, 2018a).
[c] (Yu et al., 2019).
[d] (Fujitani et al., 2017).
[e] (Janssen et al., 2014).
[f] (Saffari et al., 2014b).
[g] (Charrier et al., 2015).

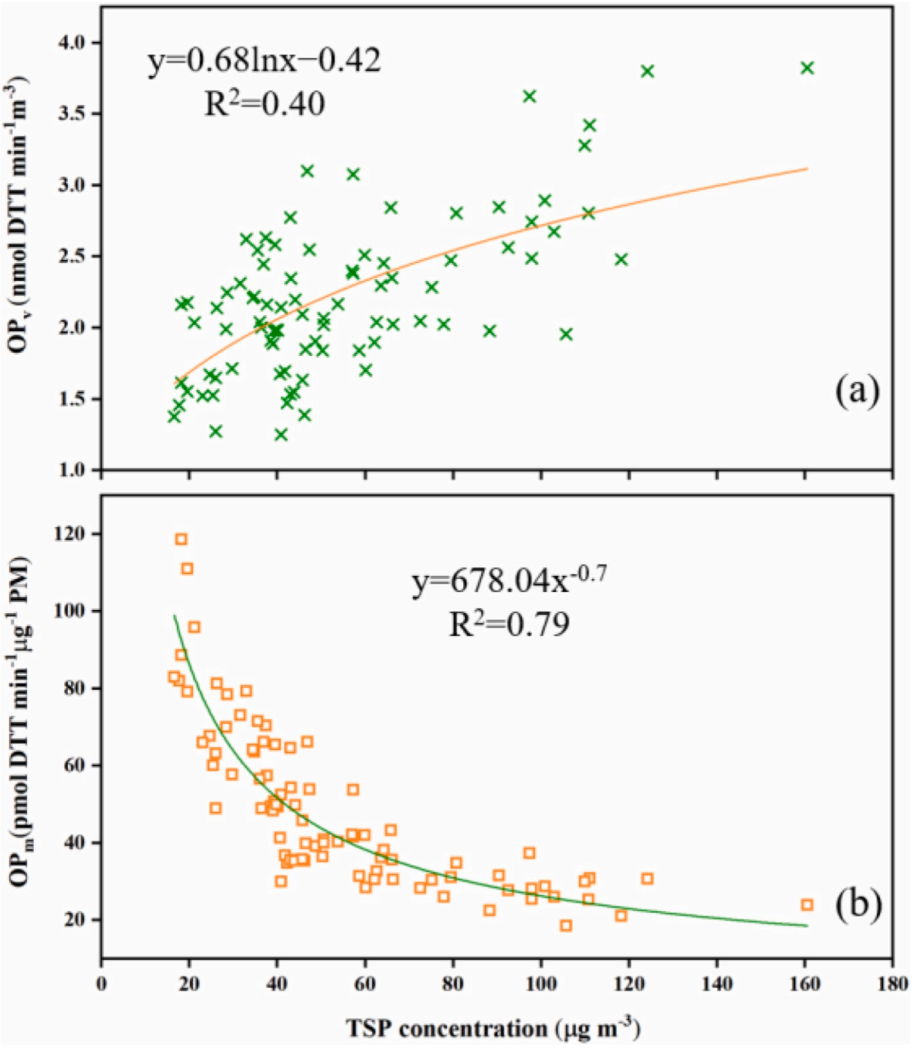

Fig. 3. Scatter plot of TSP mass concentration (μg m^{-3}) with (a) volume-normalized OP (OP_v) and (b) mass-normalized OP (OP_m).

results for species with high abundance, distinct source characteristics, relatively lower volatility, and less-reactive organics are summarized in Table S4(Wang et al., 2017). Hopanes/steranes, as well as OC and EC, were significantly and moderately correlated with OP_m (r: 0.45–0.66), indicating the importance of fossil fuel combustion on water-soluble OP in Bangkok. Moreover, the transition metals V, Ni, Cu, and Zn were moderately correlated with OP_m (r: 0.32–0.57); these metals may have originated from ship emissions, vehicle exhaust, and brake wear (Li et al., 2019). Several studies have demonstrated that transition metals can exhibit redox activity in ROS production by acting as electron mediators (Ayres et al., 2008; Charrier and Anastasio, 2012; Charrier et al., 2015; Li et al., 2019). SO_4^{2-} was moderately correlated with OP_m (r: 0.60) in this study, which was consistent with the findings of a previous study (Fang et al., 2017a). Positive correlations were also observed between non-redox-active water-soluble ions and OP_m, including K^+, Na^+, Cl^-, and Mg^{2+}(Decesari et al., 2017). However, no significant correlation was found between biomass burning tracers (e.g., levoglucosan, mannosan, and galactosan) and OP_m in this study.

3.3.2. PMF–MLR analysis and OP source apportionment

To interpret the OP_v source profiles as real-world TSP sources, we analyzed 86 TSP samples from Bangkok using the US EPA PMF5.0 model. A seven-factor solution was found to provide the most physically reasonable source profiles, recovering 96.9% of the measured TSP (Figs. S1 and S2). Ship emissions, secondary sulfate, dust, land fossil fuel combustion, sea salt, biomass burning, and industrial emissions were identified as the most influential factors through a comparison of the source profiles (details provided in Supporting Information S3). Fig. S3 shows the variation in TSP mass concentration source profiles as individual source contribution in TSP varies over time. The percent contributions of the seven PMF factors to TSP are plotted in Fig. S4. Notably, biomass burning accounted for the largest portion (mean, 26%) of TSP mass concentration.

We applied MLR analysis to predict OP_v from a linear combination of PMF-derived source contributions because it is the simplest of all acceptable statistical models that can explain the OP_v source (Bates et al., 2019; Liu et al., 2014; Yu et al., 2019; Zhang et al., 2008). The statistical metrics of the four MLR models run are listed in Table 2. Non-significant sources were excluded from the regression using a stepwise screening process to avoid overfitting ($F_{inclusion}$: $p < 0.05$; $F_{elimination}$: $p > 0.10$; Table 2). A revised model equation was run, with an adjusted r^2 of 0.936 is acquired, and all four source contributions were significantly correlated with OP_v ($p < 0.01$; Table 2, regression 4). The final optimized predictive equation was therefore established as follows:

$$OP_v = 0.113 \times \text{land fossil fuel combustion} + 0.196 \times \text{ship emissions} + 0.039 \times \text{secondary sulfate} + 0.017 \times \text{biomass burning}$$

The MLR model was determined to have moderate accuracy and sufficient model precision (Fig. S5). Model errors were consistent throughout the year and within ±40%, among which a relative deviation >40% was attributed to daily variability in the source profiles (Moschos et al., 2018). The good correlation between measured and predicted OP_v and net underestimation of annual OP_v by only 5% by the MLR model demonstrate the reliability of the model prediction of OP_v of the four sources. The OP_v prediction model reveals the sensitivity of the four significant sources. Ship emissions had the largest coefficient; thus, it was the most active source of TSP-associated OP generation, followed by land fossil fuel combustion, secondary sulfate and biomass burning.

The formulated model also provided a quantitative assessment of the four significant sources contributing to OP_v. Based on the MLR result, the time series of OP_v predicted by the four identified sources and the seasonal contribution of each source are plotted in Fig. 4. In the dry I season, fossil fuel combustion (land fossil fuel combustion [50%] + ship emissions [28%]) is the dominant contributor (78%), with additional contributions from biomass burning (11%) and secondary sulfate (11%).

Table 2
Multiple linear regression results between OP_v with individual source contributions[a].

Model	Unstandardized coefficients		Standardized coefficients	t-STAT	p-Value
	B	Standard error	Beta		
1 n = 87, r^2 = 0.873, Adj.[b] r^2 = 0.972,					
Land fossil fuel emission	0.176	0.007	0.934	24.187	0.000
2 n = 87, r^2 = 0.916, Adj. r^2 = 0.914,					
Land fossil fuel emission	0.141	0.008	0.75	17.621	0.000
Ship emissions	0.245	0.038	0.277	6.509	0.000
3 n = 87, r^2 = 0.931, Adj. r^2 = 0.929,					
Land fossil fuel emission	0.117	0.009	0.619	12.606	0.000
Ship emissions	0.244	0.034	0.275	7.128	0.000
Biomass burning	0.022	0.005	0.182	4.333	0.000
4 n = 87, r^2 = 0.939, Adj. r^2 = 0.936,					
Land fossil fuel combustion	0.113	0.009	0.6	12.849	0.000
Ship emissions	0.196	0.035	0.221	5.53	0.000
Biomass burning	0.017	0.005	0.143	3.477	0.001
Secondary sulfate	0.039	0.012	0.132	3.323	0.001

[a] Unit of source contribution is μg 3^{-1}; unit of OP_v is nmol DTT $min^{-1}m^{-3}$.
[b] Adj. r^2 indicates adjusted r^2.g.

In the wet season, the contribution of biomass burning dropped to 6%, with an increase in the contribution of land fossil fuel combustion. Land fossil fuel combustion still dominated the ROS generation potential, contributing 72% to OP_v in the dry II season, whereas ship emissions contributed relatively little (4%). Notably, secondary sulfate made relatively stable contributions to OP_v throughout the entire sampling campaign.

The seasonal contributions of various emission sources were averaged to estimate their aggregate contributions to OP_v during the entire sampling period. Land fossil fuel combustion accounted for the largest fraction of total predicted OP_v (mean: 63%; Fig. 5). Both vehicle exhaust and coal emission were also identified as land fossil fuel combustion sources; these two sources have been reported to be linked to high OP and adverse human health effects and mortality (Charrier et al., 2015; Hoffmann et al., 2007; Williams et al., 2013; Yu et al., 2019). Ship emissions are typically considered to have a negligible influence on OP_v (Bates et al., 2019). However, the contribution of ship emissions to OP_v (mean, 16%) cannot be ignored in most days in Bangkok, which is a typical harbor city in this region. The contribution of secondary sulfate (mean, 10%) determined in our study was consistent with that observed by Fang et al., who reported that sulfate plays a key role in producing highly acidic fine aerosols capable of dissolving primary transition metals that contribute to DTT activity (Fang et al., 2017a).

We applied the MLR equation to annual data and found that land fossil fuel combustion and ship emissions were the dominant contributors of water-soluble OP_v of TSP in metropolitan Bangkok. This finding is not consistent with those of several previous studies, in which biomass burning was identified as the top contributor to water-soluble OP_v of $PM_{2.5}$ in Atlanta, United States, and the main driving factor for seasonal trends of OP_v in the southeastern United States and Greece (Bates et al., 2015, 2019; Verma et al., 2014). Considering the widespread biomass burning events that occur annually in the ICP, this phenomenon may be explained by several factors. First, photochemical aerosol aging is an important factor to increase OP; therefore, proximity to biomass sources in Bangkok compared to longer transport distances in other cities (e.g., Atlanta) could affect the chemical composition (Saffari et al., 2014a; Wong et al., 2019). Second, the OP_v of TSP is likely dominated by transition metals rather than organic compounds; these metals preferentially form coarse PM, whereas organic species from biomass burning

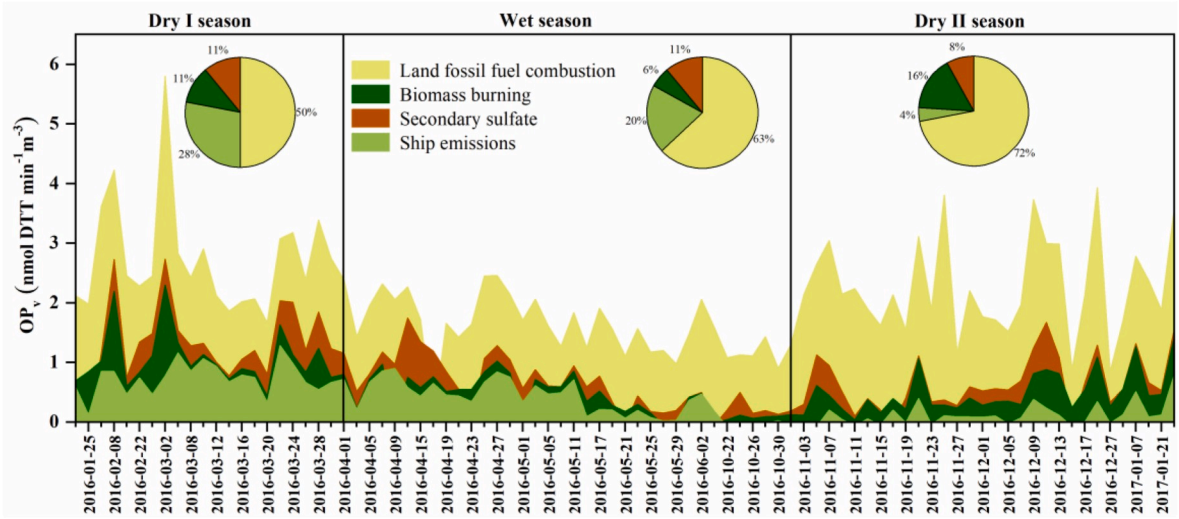

Fig. 4. The time series of water-soluble OP_v predicted by MLR model of the four identified sources and the seasonal contribution of each source.

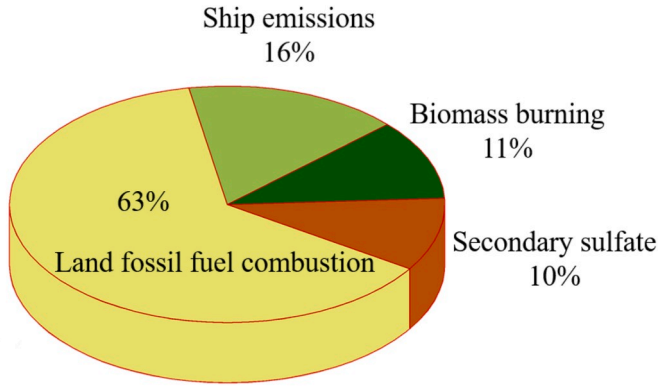

Fig. 5. The aggregate contributions of different sources identified by MLR model to water-soluble OP_v of TSP during the entire sampling campaign.

mainly form fine PM. As shown in Fig. S3, total Cu and V were the most abundant components of land fossil fuel and ship emissions, respectively.

4. Conclusion

This study is the first to examine the contributions of various emission sources to the OP of TSP in Bangkok, Thailand. The PM chemical components indicated that OM and water-soluble ions dominated the PM fractions, exhibiting noticeable variation due to greater contributions of biomass burning and fossil fuel combustion during both dry seasons. Higher concentrations of TSP mass and its associated OP_v were observed during the dry seasons than in the wet season. OP_m decreased as TSP concentration increased due to the unaccounted fractions dominating the increase in TSP and/or the inhibiting effects of redox-active metals. Additionally, OP_m was significantly correlated with transition metals (e.g., Cu, V, and Ni), hopanes/steranes, and carbonaceous species (OC and EC), indicating the influence of combustion sources, such as vehicle exhaust, ship emissions, and coal combustion, on water-soluble OP. Finally, we applied the PMF model and MLR analysis to identify and apportion the relative contributions of individual sources to the water-soluble OP of TSP. Overall, land fossil fuel combustion and ship emissions were the most important sources of water-soluble OP, with respective average contributions of 63% and 16%, followed by biomass burning (11%) and secondary sulfate (10%). We detected strong seasonality in the contributions from ship emissions and biomass burning. The formation of secondary aerosols occurred throughout the entire sampling campaign. A comparison of our results with those of previous OP studies showed that the significant contributions of fossil fuel combustion (land fossil fuel and ship emissions) to water-soluble OP were driven by transition metals Cu and V from fossil fuel combustion in TSP.

Declaration of competing interest

The authors declare that they have no known competing financial interests or personal relationships that could have appeared to influence the work reported in this paper.

CRediT authorship contribution statement

Jiaqi Wang: Conceptualization, Software, Validation, Formal analysis, Investigation, Writing - original draft, Writing - review & editing, Visualization. **Haoyu Jiang:** Methodology, Writing - review & editing. **Hongxing Jiang:** Software, Methodology, Writing - review & editing. **Yangzhi Mo:** Software, Methodology, Writing - review & editing. **Xiaofei Geng:** Software, Methodology. **Jibing Li:** Writing - review & editing. **Shuduan Mao:** Methodology. **Surat Bualert:** Resources. **Shexia Ma:** Methodology, Writing - review & editing. **Jun Li:** Resources, Data curation, Writing - review & editing, Supervision, Funding acquisition. **Gan Zhang:** Conceptualization, Resources, Data curation, Writing - review & editing, Supervision, Project administration, Funding acquisition.

Acknowledgments

Financial support was provided by the National Key R&D Program of China (2017YFC0212000), National Natural Science Foundation of China (41430645), the International Partnership Program of Chinese Academy of Sciences (132744KYSB20170002), and Guangdong Foundation for Program of Science and Technology Research (2018A050501009, 2017B030314057 and 2017BT01Z134). The authors are in debt with the students in Kasetsart University who performed with the field sampling. The original data (PMF Input Data), and output data from PMF-MRL analysis (PMF-MRL Results) could be found in SKLOG Data Repository.

Appendix A. Supplementary data

Supplementary data to this article can be found online at https://doi.

org/10.1016/j.atmosenv.2020.117624.

References

Ayres, J.G., Borm, P., Cassee, F.R., Castranova, V., Donaldson, K., Ghio, A., Harrison, R. M., Hider, R., Kelly, F., Kooter, I.M., Marano, F., Maynard, R.L., Mudway, I., Nel, A., Sioutas, C., Smith, S., Baeza-Squiban, A., Cho, A., Duggan, S., Froines, J., 2008. Evaluating the toxicity of airborne particulate matter and nanoparticles by measuring oxidative stress potential—a workshop report and consensus statement. Inhal. Toxicol. 20, 75–99.

Bates, J.T., Fang, T., Verma, V., Zeng, L.H., Weber, R.J., Tolbert, P.E., Abrams, J.Y., Sarnat, S.E., Klein, M., Mulholland, J.A., Russell, A.G., 2019. Review of acellular assays of ambient particulate matter oxidative potential: methods and relationships with composition, sources, and health effects. Environ. Sci. Technol. 53, 4003–4019.

Bates, J.T., Weber, R.J., Abrams, J., Verma, V., Fang, T., Klein, M., Strickland, M.J., Sarnat, S.E., Chang, H.H., Mulholland, J.A., Tolbert, P.E., Russell, A.G., 2015. Reactive oxygen species generation linked to sources of atmospheric particulate matter and cardiorespiratory effects. Environ. Sci. Technol. 49, 13605–13612.

Brauner, E.V., Forchhammer, L., Moller, P., Barregard, L., Gunnarsen, L., Afshari, A., Wahlin, P., Glasius, M., Dragsted, L.O., Basu, S., Raaschou-Nielsen, O., Loft, S., 2008. Indoor particles affect vascular function in the aged - an air filtration-based intervention study. Am. J. Respir. Crit. Care Med. 177, 419–425.

Brehmer, C., Lai, A., Clark, S., Shan, M., Ni, K., Ezzati, M., Yang, X.D., Baumgartner, J., Schauer, J.J., Carter, E., 2019. The oxidative potential of personal and household PM2.5 in a rural setting in southwestern China. Environ. Sci. Technol. 53, 2788–2798.

Charrier, J.G., Anastasio, C., 2012. On dithiothreitol (DTT) as a measure of oxidative potential for ambient particles: evidence for the importance of soluble transition metals. Atmos. Chem. Phys. 12, 9321–9333.

Charrier, J.G., McFall, A.S., Vu, K.K.T., Baroi, J., Olea, C., Hasson, A., Anastasio, C., 2016. A bias in the "mass-normalized" DTT response - an effect of non-linear concentration-response curves for copper and manganese. Atmos. Environ. 144, 325–334.

Charrier, J.G., Richards-Henderson, N.K., Bein, K.J., McFall, A.S., Wexler, A.S., Anastasio, C., 2015. Oxidant production from source-oriented particulate matter; Part 1: oxidative potential using the dithiothreitol (DTT) assay. Atmos. Chem. Phys. 15, 2327–2340.

Decesari, S., Sowlat, M.H., Hasheminassab, S., Sandrini, S., Gilardoni, S., Facchini, M.C., Fuzzi, S., Sioutas, C., 2017. Enhanced toxicity of aerosol in fog conditions in the Po Valley, Italy. Atmos. Chem. Phys. 17, 7721–7731.

Fang, T., Guo, H.Y., Zeng, L.H., Verma, V., Nenes, A., Weber, R.J., 2017a. Highly acidic ambient particles, soluble metals, and oxidative potential: a link between sulfate and aerosol toxicity. Environ. Sci. Technol. 51, 2611–2620.

Fang, T., Verma, V., Guo, H., King, L.E., Edgerton, E.S., Weber, R.J., 2015. A semi-automated system for quantifying the oxidative potential of ambient particles in aqueous extracts using the dithiothreitol (DTT) assay: results from the Southeastern Center for Air Pollution and Epidemiology (SCAPE). Atmos. Meas. Tech. 8, 471–482.

Fang, T., Zeng, L., Gao, D., Verma, V., Stefaniak, A.B., Weber, R.J., 2017b. Ambient size distributions and lung deposition of aerosol dithiothreitol-measured oxidative potential: contrast between soluble and insoluble particles. Environ. Sci. Technol. 51, 6802–6811.

Fujitani, Y., Furuyama, A., Tanabe, K., Hirano, S., 2017. Comparison of oxidative abilities of PM2.5 collected at traffic and residential sites in Japan. Contribution of transition metals and primary and secondary aerosols. Aerosol Air Qual. Res. 17, 574–587.

Geng, X., Zhong, G., Li, J., Cheng, Z., Mo, Y., Mao, S., Su, T., Jiang, H., Ni, K., Zhang, G., 2019. Molecular marker study of aerosols in the northern south China sea: impact of atmospheric outflow from the indo-China peninsula and south China. Atmos. Environ. 206, 225–236.

Hoffmann, B., Moebus, S., Mohlenkamp, S., Stang, A., Lehmann, N., Dragano, N., Schmermund, A., Memmesheimer, M., Mann, K., Erbel, R., Jockel, K.H., Heinz Nixdorf Recall, S., 2007. Residential exposure to traffic is associated with coronary atherosclerosis. Circulation 116, 489–496.

Janssen, N.A.H., Yang, A., Strak, M., Steenhof, M., Hellack, B., Gerlofs-Nijland, M.E., Kuhlbusch, T., Kelly, F., Harrison, R., Brunekreef, B., Hoek, G., Cassee, F., 2014. Oxidative potential of particulate matter collected at sites with different source characteristics. Sci. Total Environ. 472, 572–581.

Li, Q., Wyatt, A., Kamens, R.M., 2009. Oxidant generation and toxicity enhancement of aged-diesel exhaust. Atmos. Environ. 43, 1037–1042.

Li, X.Y., Kuang, X.B.M., Yan, C.Q., Ma, S.X., Paulson, S.E., Zhu, T., Zhang, Y.H., Zheng, M., 2019. Oxidative potential by PM2.5 in the north China plain: generation of hydroxyl radical. Environ. Sci. Technol. 53, 512–520.

Lin, M., Yu, J.Z., 2019. Effect of metal-organic interactions on the oxidative potential of mixtures of atmospheric humic-like substances and copper/manganese as investigated by the dithiothreitol assay. Sci. Total Environ. 697, 134012-134012.

Lin, P., Yu, J.Z., 2011. Generation of reactive oxygen species mediated by humic-like substances in atmospheric aerosols. Environ. Sci. Technol. 45, 10362–10368.

Liu, Q., Baumgartner, J., Zhang, Y., Liu, Y., Sun, Y., Zhang, M., 2014. Oxidative potential and inflammatory impacts of source apportioned ambient air pollution in Beijing. Environ. Sci. Technol. 48, 12920–12929.

Mao, S.D., Li, J., Cheng, Z.N., Zhong, G.C., Li, K.C., Liu, X., Zhang, G., 2018. Contribution of biomass burning to ambient particulate polycyclic aromatic hydrocarbons at a regional background site in East China. Environ. Sci. Technol. Lett. 5, 56–61.

Moschos, V., Kumar, N.K., Daellenbach, K.R., Baltensperger, U., Prevot, A.S.H., El Haddad, I., 2018. Source apportionment of Brown carbon absorption by coupling ultraviolet-visible spectroscopy with aerosol mass spectrometry. Environ. Sci. Technol. Lett. 5, 302.

Patel, A., Rastogi, N., 2018a. Oxidative potential of ambient fine aerosol over a semi-urban site in the Indo-Gangetic Plain. Atmos. Environ. 175, 127–134.

Patel, A., Rastogi, N., 2018b. Seasonal variability in chemical composition and oxidative potential of ambient aerosol over a high altitude site in western India. Sci. Total Environ. 644, 1268–1276.

Pavagadhi, S., Betha, R., Venkatesan, S., Balasubramanian, R., Hande, M.P., 2013. Physicochemical and toxicological characteristics of urban aerosols during a recent Indonesian biomass burning episode. Environ. Sci. Pollut. Control Ser. 20, 2569–2578.

Perrone, M.G., Zhou, J., Malandrino, M., Sangiorgi, G., Rizzi, C., Ferrero, L., Dommen, J., Bolzacchini, E., 2016. PM chemical composition and oxidative potential of the soluble fraction of particles at two sites in the urban area of Milan, Northern Italy. Atmos. Environ. 128, 104–113.

Pey, J., Alastuey, A., Querol, X., Rodriguez, S., 2010. Monitoring of sources and atmospheric processes controlling air quality in an urban Mediterranean environment. Atmos. Environ. 44, 4879–4890.

Saffari, A., Daher, N., Samara, C., Voutsa, D., Kouras, A., Manoli, E., Karagkiozidou, O., Vlachokostas, C., Moussiopoulos, N., Shafer, M.M., Schauer, J.J., Sioutas, C., 2013. Increased biomass burning due to the economic crisis in Greece and its adverse impact on wintertime air quality in thessaloniki. Environ. Sci. Technol. 47, 13313–13320.

Saffari, A., Daher, N., Shafer, M.M., Schauer, J.J., Sioutas, C., 2014a. Global perspective on the oxidative potential of airborne particulate matter: a synthesis of Research findings. Environ. Sci. Technol. 48, 7576–7583.

Saffari, A., Daher, N., Shafer, M.M., Schauer, J.J., Sioutas, C., 2014b. Seasonal and spatial variation in dithiothreitol (DTT) activity of quasi-ultrafine particles in the Los Angeles Basin and its association with chemical species. J. Environ. Sci. Health - Part A Toxic/Hazard. Subst. Environ. Eng. 49, 441–451.

Shiraiwa, M., Selzle, K., Poschl, U., 2012. Hazardous components and health effects of atmospheric aerosol particles: reactive oxygen species, soot, polycyclic aromatic compounds and allergenic proteins. Free Radic. Res. 46, 927–939.

Tang, J.H., Chan, L.Y., Chan, C.Y., Li, Y.S., Chang, C.C., Liu, S.C., Li, Y.D., 2007. Nonmethane hydrocarbons in the transported and local air masses at a clean remote site on Hainan Island, south China. J. Geophys. Res. Atmos. 112.

Thorpe, A., Harrison, R.M., 2008. Sources and properties of non-exhaust particulate matter from road traffic: a review. Sci. Total Environ. 400, 270–282.

Verma, V., Fang, T., Guo, H., King, L., Bates, J.T., Peltier, R.E., Edgerton, E., Russell, A. G., Weber, R.J., 2014. Reactive oxygen species associated with water-soluble PM2.5 in the southeastern United States: spatiotemporal trends and source apportionment. Atmos. Chem. Phys. 14, 12915–12930.

Wang, Q.Q., He, X., Huang, X.H.H., Griffith, S.M., Feng, Y.M., Zhang, T., Zhang, Q.Y., Wu, D., Yu, J.Z., 2017. Impact of secondary organic aerosol tracers on tracer-based source apportionment of organic carbon and PM2.5: a case study in the Pearl river Delta, China. Acs Earth Space Chem. 1, 562–571.

Williams, E.S., Mahler, B.J., Van Metre, P.C., 2013. Cancer risk from incidental ingestion exposures to PAHs associated with coal-tar-sealed pavement. Environ. Sci. Technol. 47, 1101–1109.

Wong, J.P.S., Tsagkaraki, M., Tsiodra, I., Mihalopoulos, N., Violaki, K., Kanakidou, M., Sciare, J., Nenes, A., Weber, R.J., 2019. Effects of atmospheric processing on the oxidative potential of biomass burning organic aerosols. Environ. Sci. Technol. 53, 6747–6756.

Xing, L., Fu, T.M., Cao, J.J., Lee, S.C., Wang, G.H., Ho, K.F., Cheng, M.C., You, C.F., Wang, T.J., 2013. Seasonal and spatial variability of the OM/OC mass ratios and high regional correlation between oxalic acid and zinc in Chinese urban organic aerosols. Atmos. Chem. Phys. 13, 4307–4318.

Yadav, I.C., Devi, N.L., Li, J., Syed, J.H., Zhang, G., Watanabe, H., 2017. Biomass burning in Indo-China peninsula and its impacts on regional air quality and global climate change-a review. Environ. Pollut. 227, 414–427.

Yu, S.Y., Liu, W.J., Xu, Y.S., Yi, K., Zhou, M., Tao, S., Liu, W.X., 2019. Characteristics and oxidative potential of atmospheric PM2.5 in Beijing: source apportionment and seasonal variation. Sci. Total Environ. 650, 277–287.

Zelikoff, J.T., Chen, L.C., Cohen, M.D., Schlesinger, R.B., 2002. The toxicology of inhaled woodsmoke. J. Toxicol. Environ. Health B Crit. Rev. 5, 269–282.

Zhang, G., Li, J., Li, X.D., Xu, Y., Guo, L.L., Tang, J.H., Lee, C.S.L., Liu, X.A., Chen, Y.J., 2010. Impact of anthropogenic emissions and open biomass burning on regional carbonaceous aerosols in South China. Environ. Pollut. 158, 3392–3400.

Zhang, N., Cao, J., Liu, S., Zhao, Z., Xu, H., Xiao, S., 2014. Chemical composition and sources of PM2.5 and TSP collected at Qinghai Lake during summertime. Atmos. Res. 138, 213–222.

Zhang, Y.X., Schauer, J.J., Shafer, M.M., Hannigan, M.P., Dutton, S.J., 2008. Source apportionment of in vitro reactive oxygen species bioassay activity from atmospheric particulate matter. Environ. Sci. Technol. 42, 7502–7509.